Chemical Science

ROYAL SOCIETY OF CHEMISTRY

EDGE ARTICLE

View Article Online
View Journal | View Issue

Cite this: *Chem. Sci.*, 2025, **16**, 6257

All publication charges for this article have been paid for by the Royal Society of Chemistry

Fluoride-induced redox-switchable behaviour of a palladium(II)/(IV) couple†

Sebastián Martínez-Vivas, Macarena Poyatos * and Eduardo Peris *

We report the preparation of two Pd(II) complexes based on (CCC)-pincer-NHC (NHC = N-heterocyclic carbene) ligands. One of these complexes features an NDI unit (NDI = naphthalene-diimide) attached to the CCC-pincer ligand. Reacting these complexes with bromine results in the formation of the corresponding palladium(IV) complexes [$PdBr_3$(NDI-CCC)] and [$PdBr_3$(CCC)]. The NDI-containing pincer complex exhibits a strong sensitivity to fluoride ions, which can induce a one-electron reduction of the naphthalene-diimide moiety. We demonstrate that the addition of fluoride induces the reduction of the NDI moiety *via* the formation of hydroxide anions, which are the effective reducing agents of the process. The addition of fluoride significantly affects the reactivity of the NDI-containing palladium complexes. For example, the palladium(IV) complex [$PdBr_3$(NDI-CCC)] can transfer bromide to styrene in a stoichiometric manner, but this reaction is inhibited in the presence of fluoride. Similarly, the palladium(II) complex [PdI(NDI-CCC)] catalyzes the oxidative homocoupling of arylpyridines, but its catalytic activity is quenched when excess fluoride is added. Notably, we demonstrate that this process can be deactivated and reactivated by sequentially introducing an excess of fluoride and $NOBF_4$, revealing a rare instance of a redox-switchable process within a Pd(II)/Pd(IV) catalytic cycle. In contrast, the (CCC)-pincer palladium(II) and (IV) complexes lacking the NDI unit show no sensitivity to fluoride. Our study demonstrates that a simple reagent, such as the fluoride anion, can effectively modulate the reactivity of the Pd(II)/Pd(IV) pair. More broadly, it shows that fluoride serves as a simpler alternative to the metal-based reducing agents commonly used in redox-switchable catalysis.

Received 3rd December 2024
Accepted 7th March 2025

DOI: 10.1039/d4sc08203f

rsc.li/chemical-science

Introduction

Palladium(IV) complexes have been increasingly recognized as intermediates in many catalytic reactions,[1] but these species were initially viewed with skepticism owing to a lack of evidence supporting their viability. This is because high-valent Pd compounds were traditionally considered very unstable under ambient conditions, as they tend to undergo rapid decomposition *via* reductive elimination processes. Exploiting Pd(II)/Pd(IV) catalysis brings new opportunities in terms of mechanistic information and catalytic applications, because it provides complementary reactivities that are unattainable for Pd(0)/Pd(II) couples.[2] Compared to Pd(0)/Pd(II) catalysis, Pd(II)/Pd(IV) processes benefit from the resistance of Pd(IV) species to undergo β-H elimination, and because Pd(IV) compounds undergo facile reductive elimination. This explains why high-valent palladium complexes promote facile carbon–halogen bond-forming reductive elimination, while this process is both kinetically and thermodynamically unfavorable from Pd(II) complexes. The impressive recent advances in Pd(II)/Pd(IV) catalysis related to carbon–halogen bond formation[3] and C–H activation[1b,4] have stimulated detailed studies to unveil the factors that dictate the energetics of oxidative addition at palladium(II), and reductive elimination from palladium(IV) complexes.[1d,2,5]

It is now widely recognized that Pd(IV) complexes can be stabilized by using rigid multidentate strong electron-donating ligands,[2,6] among which bis-chelating[3a,b] and pincer NHC-based[5a,7] ligands (NHC = N-heterocyclic carbene) are gaining increasing attention. We have been recently interested in studying how oxidative addition processes at NHC-based pincer rhodium(I) complexes can be controlled by using supramolecular interactions,[8] or by the addition of halides.[9] In particular, we observed that pincer-NHC-based ligands functionalized with naphthalene-diimides (NDIs) are highly sensitive to the addition of fluoride or chloride,[9,10] and this has a strong influence on the catalytic performance of their related metal complexes. Our studies were based on the fact that NDI-containing compounds are known to engage in strong anion–π interactions,[11] thus we

Institute of Advanced Materials (INAM), Centro de Innovación en Química Avanzada (ORFEO-CINQA), Universitat Jaume I, Av. Vicente Sos Baynat s/n, Castellón, E-12071, Spain. E-mail: poyatosd@uji.es; eperis@uji.es

† Electronic supplementary information (ESI) available: Experimental details dealing with the characterization, electrochemical and spectroelectrochemical measurements, reactivity studies and catalytic experiments. The data related to the crystallographic studies. CCDC 2387767, 2387768 and 2387900. For ESI and crystallographic data in CIF or other electronic format see DOI: https://doi.org/10.1039/d4sc08203f

initially hypothesized that the combination of pincer ligands with NDIs should constitute an effective way of designing anion-sensitive pincer ligands, which could be further used for approaching new catalytic transformations or for facilitating the stabilization of metal complexes in high oxidation states. In two previous studies, we demonstrated how the addition of halides can be used to modulate the electron-donating strength of NDI-functionalized bis-NHC pincer ligands, thereby influencing the electron richness of the metal centers to which they are bound.[9,10] Building on this foundation, we now synthesized two NDI-functionalized (CCC)- and (CNC)-NHC-based pincer complexes of Pd(II), and approached the preparation of their related Pd(IV) complexes by oxidation with molecular bromine. We thought that the stability conferred to the Pd(IV) complex by the rigid NDI-functionalized tridentate pincer ligand could be modulated by increasing the electron donating strength of the ligand by addition of the fluoride anion.[9] As we describe herein, the reactivity and catalytic properties of the reported NDI-functionalized pincer complexes of Pd(IV) are highly influenced by the addition of fluoride.

Results and discussion

Scheme 1 shows the synthetic procedure for the preparation of the three Pd(II) bis-NHC complexes **4–6**, which are described in the present study. The NDI-functionalized (CCC)-pincer palladium complex **4** was obtained by reaction of the NDI-substituted phenyl bisimidazolium salt [**1**](I)$_2$ with palladium acetate in the presence of sodium acetate in DMSO at 140 °C (40% yield). By using the same synthetic procedure, but using the methyl-substituted phenyl-bisimidazolium salt [**2**](I)$_2$, (CCC)-pincer complex **5** was obtained in 45% yield. The (CNC) pincer complex **6** was prepared by reacting the pyridyl-bisimidazolium salt [**3**](I)$_2$ with silver oxide in CH_2Cl_2, and then by transmetalating the *in situ* preformed silver-NHC complex with [$PdCl_2$(COD)] in the presence of Na(BAr^F_4). All three Pd(II) complexes were characterized by NMR spectroscopy and mass spectrometry (see the ESI† file for full details). All three complexes are very stable in solution and in the solid state for long periods of time.

The structure of the (CNC)-pincer complex **6** was further verified by single crystal X-ray diffraction studies (Fig. 1). The structure shows the pincer coordination of the pyridyl-bis-NHC ligand, which establishes a Pd–N distance of 1.995(6) Å, and Pd–C distances of 2.044(8) and 2.061(7) Å. The angle between the plane formed by the pincer ligand and the NDI moiety is 67.75°. The longer axis of the NDI moiety and the Cl–Pd–N axis establish an angle of 163.54°, thus slightly deviating from linearity.

In order to prepare the related pincer complexes of Pd(IV), three equivalents of Br_2 were added to solutions of complexes **4–6** in CH_2Cl_2, and the resulting mixtures were allowed to react for five minutes at room temperature (see Scheme 2). Under these mild reaction conditions, both **4** and **5** evolved to their related Pd(IV) tribromide complexes **7** and **8**, which were obtained in very high yield (>80%). These tribromide complexes were obtained regardless of the presence of the iodo ligands in **4** and **5**. The NDI-containing pincer complex of Pd(IV) **7** was also obtained from the preformed pincer Pd–Br complex **9**, which was obtained at room temperature by reaction of **4** with an excess of NaBr in acetone. Complexes **7** and **8** were characterized by NMR spectroscopy and mass spectrometry (see the ESI† file for full details). Complex **7** showed great stability in the solid state and in solution, while **8** tended to decompose at room temperature in hours in a solution of chlorinated solvents such as $CHCl_3$ or CH_2Cl_2. The (CNC)-pincer palladium(II) complex **6** did not produce the desired Pd(IV) complex under these reaction conditions, or even when the reaction was allowed to proceed for a longer reaction time or at higher temperatures. While all Pd(II) complexes **4–6** contain rigid strong electron-donating pincer bis-NHC ligands, the unattainability of the targeted Pd(IV) from **6** is most likely related to the lower electron richness of the metal center due to the cationic nature of the complex. This may also be the reason why Pd(IV) with (CNC)-pincer bis-NHC complexes have not been reported so far.

The molecular structure of **7** was confirmed by means of single crystal X-ray diffraction studies. The structure (Fig. 2) consists of a phenylene-bis-imidazolylidene ligand with an appended NDI moiety coordinated to palladium in a pincer fashion. Three bromo ligands complete the pseudo-octahedral coordination sphere about the palladium center. The NDI moiety is disposed in a quasiperpendicular orientation with respect to the equatorial plane of the complex, as shown by the angle established between these two planes, which measures 82.5°. The Pd–$C_{carbene}$ distances measure 1.966(9) and 2.074(8) Å, while the Pd–Br distances are 2.4694(11), 2.4619(12) and 2.5649(12) Å, the latter one being the one assigned to the bromo

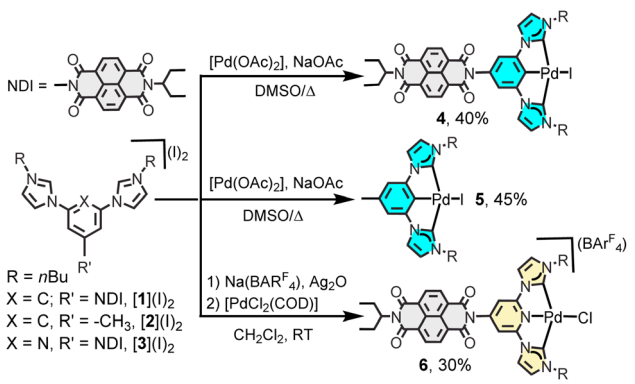

Scheme 1 Synthesis of pincer-bis(NHC) Pd(II) complexes.

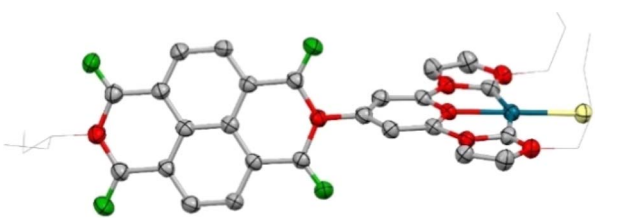

Fig. 1 Molecular structure of complex **6**. Hydrogen atoms and counter anion (BAr^F_4) are omitted for clarity. Carbon atoms in grey, palladium in blue, nitrogen atoms in red, chlorine atom in yellow and oxygen atoms in green.

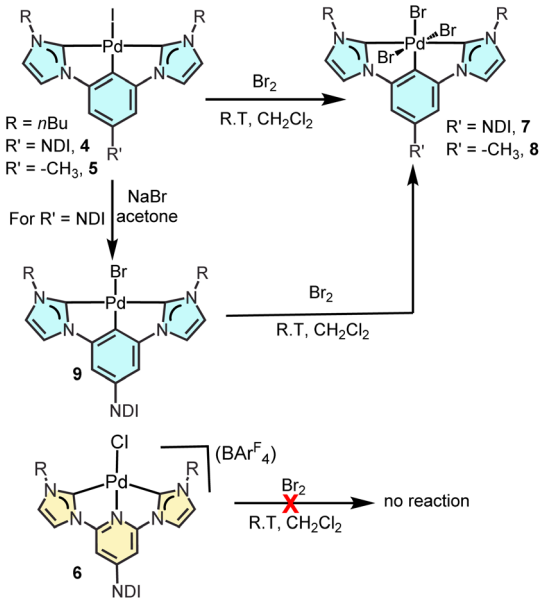

Scheme 2 Oxidation of Pd(II) complexes with bromine.

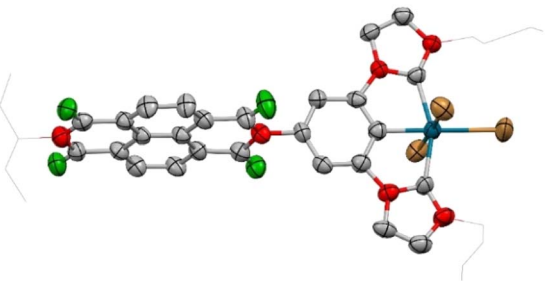

Fig. 2 Molecular structure of complex **7**. Hydrogen atoms and solvent molecules (CH_2Cl_2) were omitted for clarity. Carbon atoms in grey, palladium in blue, nitrogen atoms in red, oxygen atoms in green and bromine atoms in brown.

ligand *trans* to the phenylene ring, whose longer distance is attributed to the trans influence exerted by the aryl ligand.

Given that NDIs are known to be sensitive to the addition of halides, we decided to compare the reactivity of **7** and **8** towards the addition of tetrabutyl ammonium fluoride (TBAF). It is well known that the addition of fluoride to NDI induces the reduction of NDI to the radical anion $NDI^{\bullet-}$ and sometimes to the dianion NDI^{2-}.[12] During some time the ability of fluorides to reduce NDIs was a matter of controversy, but some detailed studies by Gabbai and co-workers proposed that, in the presence of solvents with protons (*e.g.* acetonitrile, DMSO, DMF), the deprotonated solvent is the actual electron donor for the reduction of NDI.[12b] More recently, two independent studies by Ghosh[12d] and Tam and Xu[12e] proved that, in the absence of protic solvents, fluoride reacts with water (coming from commercial $TBAF\cdot 3H_2O$) forming the very stable difluoride anion HF_2^-. The OH^- anion thus produced forms an anion–π complex with the NDI unit, and then the electron transfer from OH^- to NDI is produced facilitating the formation of $NDI^{\bullet-}$ and finally NDI^{2-}.[12d]

Fig. 3 shows the series of spectra obtained from the reaction of complex **7** upon addition of increasing amounts of TBAF in DMSO-d_6. As can be observed from these spectra, the addition of TBAF produces the gradual formation of Pd(II) complex **9**. Four equivalents of TBAF are needed for the complete transformation of **7** into **9**. This stoichiometry is consistent with previous studies that suggest that two equivalents of fluoride are needed to deprotonate water to form OH^- and HF_2^-, with OH^- performing the electron transfer process to NDI.[12b,d,e] As two electrons are needed in the reduction of Pd(IV) to Pd(II), the whole reduction process requires four equivalents of fluoride. Further addition of TBAF (five equivalents) results in the disappearance of the proton resonances due to the formation of a paramagnetic species, which can be attributed to the reduction of the NDI unit to $NDI^{\bullet-}$ radical in $\mathbf{9}^{\bullet-}$. Subsequent addition of two equivalents of $NOBF_4$ allowed the reoxidation of $\mathbf{9}^{\bullet-}$ to **9** (Fig. 3, bottom spectrum), thus showcasing the reversibility of the process.

Under the same conditions, the addition of increasing amounts of TBAF over a DMSO-d_6 solution of Pd(IV) complex **8** showed that this Pd(IV) is perfectly stable in the presence of fluoride (no changes were observed in the resulting ^{1}H NMR spectra, see Fig. S41 in the ESI† for details), thus indicating that the presence of the NDI unit is needed to induce the reduction of Pd(IV) to Pd(II). To determine whether a direct connection between the NDI unit and the metal center is required for the reduction of Pd(IV), we conducted an experiment in which an equimolar mixture of compound **8** and *N*,*N*′-di-(1-ethylpropyl)-naphthalene-diimide was reacted with four equivalents of TBAF in DMSO-d_6. The ^{1}H NMR spectra revealed that the resonances of the NDI protons disappeared, indicating the formation of $NDI^{\bullet-}$. However, the signals corresponding to compound **8** remained unchanged (see Fig. S42 in the ESI† for

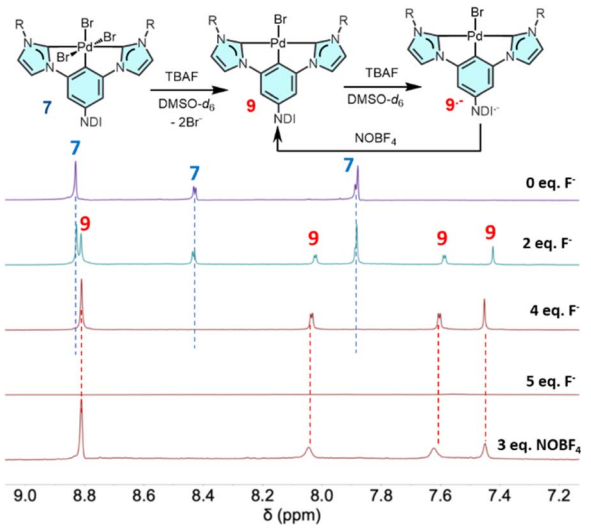

Fig. 3 Selected region of the ^{1}H NMR spectra of complex **7** in DMSO-d_6 upon the addition of increasing amounts of $TBAF\cdot 3H_2O$ showing the formation of the Pd(II) complex **9**, and finally the paramagnetic species $\mathbf{9}^{\bullet-}$. Subsequent addition of $NOBF_4$ reoxidizes $\mathbf{9}^{\bullet-}$ to **9** (bottom spectrum).

details). This control experiment demonstrates that a direct connection between the NDI unit and the metal is essential for Pd(IV) reduction, and that the electron transfer between the NDI unit and the metal is intramolecular.

In contrast, when either compound **8** or compound **7** was reacted with two equivalents of cobaltocene (Cp_2Co), both complexes were readily reduced to their corresponding Pd(II) forms, the bromo-analogue of **5** and **9**, respectively (see Fig. S43 in the ESI for details†). Further addition of two equivalents of Cp_2Co to compound **9** led to the reduction of the NDI moiety, forming **9**$^{\bullet-}$. These experiments highlight that, while Cp_2Co promotes the indiscriminate reduction of both Pd(IV) complexes, TBAF can be used as a more selective additive to reduce only those complexes containing the NDI unit.

In order to shed some light into the mechanism of the reduction of the NDI-containing Pd(IV) complex **7** into the Pd(II) complex **9**, we performed a series of electrochemical and spectroelectrochemical studies. The cyclic voltammetry of complex **7** shows one irreversible cathodic peak at −0.502 V (*vs.* Fc+/Fc), and two reversible waves at −1.00 and −1.44 V (see Fig. S31 and S32 in the ESI† for details). The first reduction event at −0.502 V is attributed to the one electron reduction of the palladium(IV) center, while the two reversible waves at more negative potentials are due to the one- and two electron reductions of the NDI unit. This experiment indicates that, as the HOMO level of NDI$^{\bullet-}$ lies above the LUMO of Pd(IV), once the fluoride anion induces the reduction of NDI, then an electron transfer occurs between NDI$^{\bullet-}$ and the metal center facilitating the reduction of Pd(IV). In the absence of the NDI unit, this process does not occur, and this explains the absence of reactivity between **8** and fluoride.

In order to confirm that the addition of fluoride induces the reduction of the NDI unit, we compared the series of spectra resulting from the UV-Vis spectroelectrochemical (SEC) experiments, and from the UV-Vis titration of **4** with TBAF in DMSO. The spectra resulting from both experiments are shown in Fig. 4. As can be observed from Fig. 4a, the UV-vis spectrum of complex **4** shows a vibronically-resolved band centered at 380 nm, which is attributed to transitions centered at the NDI unit. Upon applying a negative potential of −1200 mV, this band reduces its intensity and new featureless bands centered at 470 and 620 nm appear, which are consistent with the appearance of the one-electron reduced species [PdI(CCC-NDI$^{\bullet-}$)] (**4**$^{\bullet-}$). When more negative potentials are applied (V_{ap} = −1600 mV), a further decrease of the intensity of the band at 380 nm is observed, with the concomitant appearance of two bands at 710 and 770 nm, thus confirming the complete formation of **4**$^{\bullet-}$. A very similar situation is produced when fluoride is added over a solution of **4** in DMSO. As can be observed in Fig. 4b, the addition of five equivalents of TBAF produced a species whose UV-Vis spectrum is quasi-identical to that obtained from the electrochemical one-electron reduction of **4**, thus strongly suggesting that [PdI(CCC-NDI$^{\bullet-}$)] (**4**$^{\bullet-}$) was formed. Further addition of TBAF (up to 10 equivalents) results in the quantitative formation of (**4**$^{\bullet-}$). This experiment shows that the NDI unit at **4** can be reduced by one electron upon addition of a large excess of fluoride, in agreement with

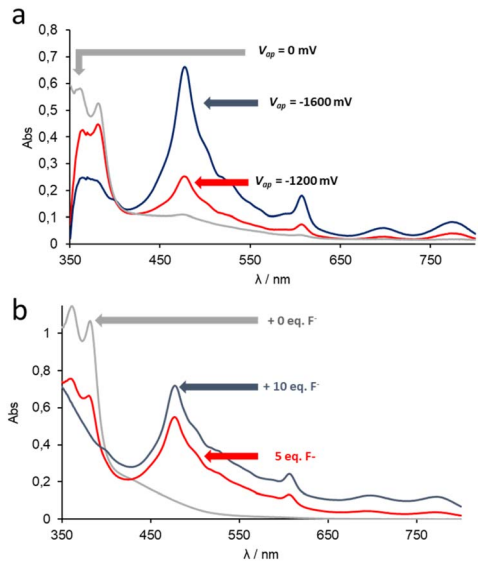

Fig. 4 (a) UV-Vis-SEC monitoring reduction of **4** in dry DMSO (0.25 M [N(nBu)$_4$][PF$_6$]). The solid lines represent the UV-Vis spectra of complex **4** (grey), the partial formation (red) and the complete formation (blue) of the one-electron reduced species **4**$^{\bullet-}$. (b) UV-Vis spectroscopic changes in the spectrum of **4** observed upon the addition of different amounts of TBAF·3H$_2$O [0 equivalents of TBAF (grey); 5 equivalents of TBAF (red); 10 equivalents of TBAF (blue)].

previous studies.[12d,e] In order to check if the addition of OH$^-$ anions would produce a similar effect on the reduction of the NDI unit, we also carried out a reaction between **4** and TBAOH. As can be observed in Fig. S38 of the ESI,† the addition of two equivalents of TBAOH to a DMSO-d_6 solution of **4** results in the disappearance of the proton resonances due to the formation of a paramagnetic species, whose UV-Vis spectrum matches perfectly with that of **4**$^{\bullet-}$. This experiment aligns with all previous studies suggesting that the reduction of the NDI unit by the fluoride anion proceeds through the OH$^-$–π complex with the NDI moiety.[12b,d,e]

We next decided to evaluate the effect of the addition of fluoride on the bromine transfer reaction to styrene. The stoichiometric halogen transfer reactions from Pd(IV) halide-containing complexes to olefins and alkynes have been previously reported by Kraft[3a,b] and Guo,[5a] and constitute a process that exemplifies the high tendency of Pd(IV) complexes to form carbon–halogen bonds. The reactions were carried out in a sealed NMR tube at 80 °C in $CDCl_3$, using an excess of 5 equivalents of styrene, and the conversion was determined by ^{1}HNMR spectroscopy based on the formation of the corresponding Pd(II) complexes and in the formation of the related amount of 1,2-dibromoethylbenzene. As can be observed from the time-dependent reaction profiles shown in Fig. 5, after 10 h of reaction the bromine transfer process is produced in 70% for complex **7**, while complex **8** only reaches 50% conversion. More interesting is the fact that, in the presence of five equivalents of TBAF, the NDI-containing Pd(IV) complex **7** does not cause the formation of 1,2-dibromoethylbenzene, while under the same reaction conditions **8** shows exactly the same bromination capacity as in the absence of TBAF. This result shows that the

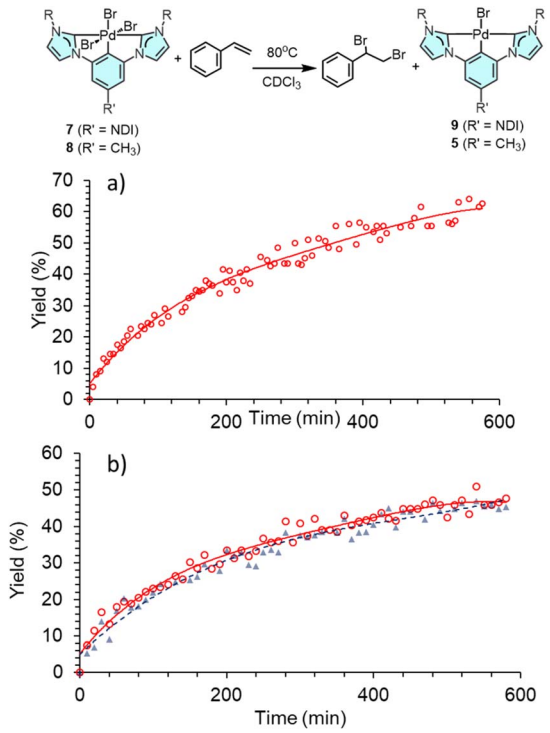

Fig. 5 Time-dependent reaction profiles of the bromine transfer reaction from (a) complex **7** and (b) complex **8**, to styrene. The reactions were monitored by ^{1}H NMR spectroscopy, by recording the corresponding spectra every 5 minutes. The red empty dots represent evolution of the reaction carried out in the absence of fluoride. The blue triangles in (b) represent the evolution of the reaction in the presence of 5 equivalents of TBAF for the reaction carried out with **8**. Addition of 5 equivalents of TBAF to the reaction performed with **7** shows no formation 1,2-dibromoethylbenzene.

bromination abilities of **7** can be quenched in the presence of the fluoride anion, as a consequence of its reduction from Pd(IV) to Pd(II).

We also wanted to test if the addition of fluoride could have any effect on the catalytic properties of the two Pd(II) complexes under study. As a model reaction, we studied the oxidative homocoupling of 2-arylpyridines. This reaction has been studied for almost two decades using Pd,[13] Cu,[14] Ru[15] and Co[16]-based homogeneous catalysts in combination with various oxidants. The process is considered to be the first evidence of a Pd(IV) mediated C–H bond activation.[13a] Based on the well-accepted mechanism for the Pd-catalysed dehydrogenative homocoupling of aryl-pyridines, the reaction proceeds through a Pd(II)/Pd(IV) mechanism which involves two distinct C–H activation steps [one at Pd(II) and the other at Pd(IV)] followed by the reductive elimination of the final homocoupled product.[13a] We first performed the reactions at room temperature using catalysts **4** and **5** (5 mol%) using a 0.11 M solution of 2-phenylpyridine in CD_3CN, and using $NO^+BF_4^-$ and I_2 as oxidants to promote the Pd(II)–Pd(IV) step. Neither of these two oxidants facilitated the homocoupling process under these reaction conditions. Then, we performed the reactions using complexes **4** and **5** as catalysts under the same reaction conditions using selectfluor (0.66 mmol) as oxidant. We decided to use selectfluor because this reagent has been used widely as an oxidant of transition metals, especially for facilitating catalytic processes involving selective oxidative C–H functionalization,[17] and it has also been used to facilitate the oxidative homocoupling of arenes using palladium(II) complexes with pincer-type ligands.[18] As mentioned before, all reactions were performed at room temperature and their progress was monitored by ^{1}H NMR spectroscopy. Under these conditions, the reactions followed zeroth order kinetics with respect to phenyl-pyridine (see Fig. S47 in the ESI† for details). This most likely indicates that the substrate is coordinated to the metal in the resting state of the process, and that the product is not released from the coordination sphere of the complex in the rate-determining step (RDS) of the cycle. With this data in hand, the oxidation from Pd(II) to Pd(IV) is most likely the RDS of the catalytic cycle. Analysis of the reaction rates at three different catalyst concentrations allowed us to determine that the reaction follows first order kinetics with respect to the catalyst (see Fig. S46 in the ESI† for details). Complexes **4** and **5** show quasi-identical reaction rates for the dimerization of 2-phenyl pyridine [$(2.8 \pm 0.1) \times 10^{-6}$ and $(3.0 \pm 0.1) \times 10^{-6}$ M s^{-1}, for **4** and **5** respectively]. We next wanted to test the effect of the addition of TBAF on the reaction rate of this process. The reactions were performed using both catalysts **4** and **5**, under the same standard reaction conditions (5 mol% of catalyst loading, room temperature in CD_3CN), but with the addition of five equivalents of TBAF with respect to the catalyst. As can be observed in the reaction profiles shown in Fig. 6a and b, the addition of TBAF on the reaction carried out with **5** did not have any effect on the reaction rate, while the rate for the reaction carried out with the NDI-appended catalyst **4** was reduced by a factor of 0.5 when 5 equivalents of fluoride were added. This partial inhibition of the catalytic activity of **4** could be due to the partial reduction of the NDI moiety of the catalyst, in agreement with the UV-Vis spectroscopic changes observed upon addition of fluoride as discussed above (Fig. 4b), which showed that the addition of 5 equivalents of TBAF was not enough to produce the complete reduction of NDI. With this result in hand, we performed another reaction using catalyst **4** and added ten equivalents of TBAF. Under these reaction conditions, the catalytic activity of **4** was almost completely quenched, as the reaction rate is five times slower than in the absence of fluoride, as can be observed in Fig. 6b.

Finally, we wanted to see if the influence of fluoride addition on the activity of **4** was reversible. In order to do this, we performed an experiment in which we followed the homocoupling of 2-phenylpyridine using catalyst **4**, and then we sequentially added ten equivalents of TBAF and $NO^+BF_4^-$. As can be observed in the reaction profile shown in Fig. 7, the addition of TBAF induced the complete inhibition of the activity of the catalyst, which was fully recovered after addition of ten equivalents of $NO^+BF_4^-$. With these results in hand, a question that remains is whether the catalytic switchable behavior is facilitated by the $NDI^{\bullet-}$/NDI redox couple or the Pd(II)/Pd(IV) couple, as the process is facilitated by sequentially adding a reducing agent (or in this case fluoride, which acts as a proxy of a reducing reagent), and an oxidant (NO^+) which, in principle,

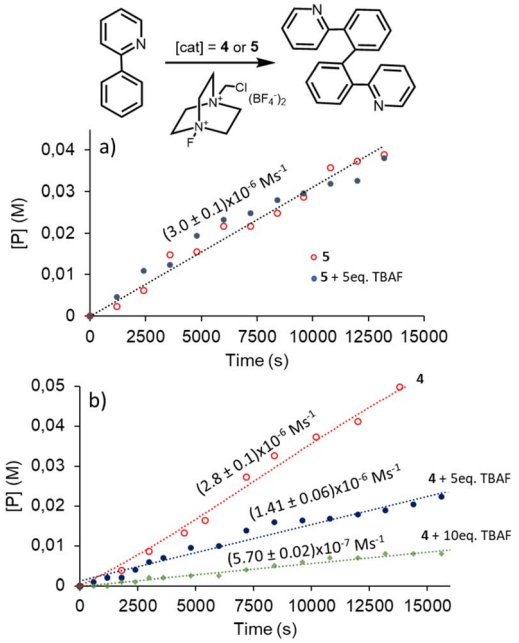

Fig. 6 Time-dependent reaction profiles of the catalytic dehydrogenative homocoupling of 2-phenylpyridine using **5** (a) and **4** (b) as catalysts. Red empty dots represent the profiles for the reactions using the catalysts (5 mol%) in the absence of additives. Blue solid dots and green squares represent the profiles for the reactions carried out with the catalyst +5 and +10 equivalents of TBAF, respectively. All reactions were performed in CD_3CN at room temperature, and the evolution was monitored by ^1H NMR spectroscopy.

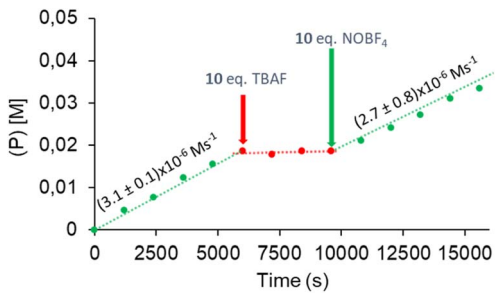

Fig. 7 Time-dependent reaction profile of the catalytic dehydrogenative homocoupling of 2-phenylpyridine initiated with **4** as catalyst (5 mol%), and then deactivated and re-activated by sequentially adding TBAF (10 equivalents with respect to the catalyst) and $NO^+BF_4^-$ (10 equivalents with respect to the catalyst). The reaction was performed in CD_3CN at room temperature. Product yields determined by ^1H NMR spectroscopy.

could have an effect on both redox pairs. The answer to this question can be found in the following experimental results: (i) the inhibition of the activity of the catalyst is explained as a consequence of the one-electron reduction of the NDI moiety at the catalyst, which avoids the formation of the Pd(IV) species (catalyst **5**, lacking the NDI unit, is not affected by the addition of fluoride); (ii) the recovery of the activity of the catalyst after the addition of $NO^+BF_4^-$ is due to the reoxidation of the $NDI^{\bullet-}$ radical formed after addition of fluoride, because NO^+ is not a strong enough oxidant to facilitate the Pd(II)–Pd(IV) step (as we mentioned before, the homocoupling reaction does not work when NO^+ alone is used as an oxidant); (iii) selectfluor, while being an oxidant, does not seem to react with the one-electron reduced NDI unit, as it is not consumed after addition of ten equivalents of TBAF; and (iv) after reactivating the catalyst upon addition of $NO^+BF_4^-$, the Pd(II)–Pd(IV) step of the catalytic cycle is facilitated by selectfluor, which remains the active transition metal oxidant. All this means that all the fluoride-induced redox-switchable properties of **4** are centered at the NDI unit rather than at the Pd center.

In order to further explore the scope of **4** in the coupling of aryl-pyridines, we also tested its activity in the homocoupling of substituted phenyl pyridines, such as 2-(*p*-tolyl)-pyridine and 2-(*p*-methoxyphenyl)-pyridine and also phenanthroline, where it produced the expected homocoupling products with yields ranging from 80–90% after 12 h of reaction, except for 2-(*p*-tolyl)-pyridine, which was converted into its dimer in only 52% yield.

Conclusions

In summary, we synthesized three different bis-NHC-based pincer complexes of Pd(II) and demonstrated how oxidation to their corresponding Pd(IV) complexes was strongly influenced by the type of pincer ligand coordinated to the metal. The neutral Pd(II) complexes with a phenylene-bis-NHC pincer ligand were easily oxidized to their related $[PdBr_3(CCC)]$ Pd(IV) complexes upon reaction with Br_2. In contrast, the Pd(II) complex with a pyridyl-bis-NHC pincer ligand showed limited oxidation to Pd(IV), likely due to the lower electron richness of the metal in the cationic complex.

We also investigated the reactivity of the $[PdBr_3(CCC)]$ Pd(IV) complexes, which varied significantly depending on whether the (CCC)-pincer ligand was attached to an NDI unit or not. Upon the addition of an excess of fluoride, the NDI-containing complex **7** was rapidly reduced to its corresponding Pd(II) complex **9**, with the formula [PdBr(NDI-CCC)]. In contrast, compound **8**, which lacks the NDI unit, remained stable even in the presence of an excess of fluoride. The sensitivity of **7** to fluoride was further demonstrated in two model reactions with organic substrates. The bromine transfer from **7** to styrene was completely inhibited by an excess of fluoride, and while both **4** and **5** were active catalysts in the dehydrogenative homocoupling of 2-arylpyridines, only the activity of **4** was inhibited by an excess of fluoride.

These observations suggest that fluoride induces the reduction of the NDI unit in the catalyst, which is followed by two successive electron transfers from the NDI anion ($NDI^{\bullet-}$) to Pd(IV), leading to the reduction of Pd(IV) to Pd(II). It is also important to note that, consistent with previous studies,[12b,d,12e] our work provides additional experimental evidence supporting the idea that fluoride anions reduce NDI through the formation of hydroxide anions. These hydroxide anions then form an OH^-–π complex with the NDI moiety, facilitating electron transfer from OH^- to NDI and promoting the formation of the $NDI^{\bullet-}$ radical.

In practical terms, our findings demonstrate that the redox transition between the Pd(II)/Pd(IV) couple can be easily modulated by adding fluoride to NDI-containing complexes, providing a novel approach to control this critical chemical step. Additionally, our results highlight how combining NDI units with metal complexes can reveal new reactivity patterns that have yet to be explored. This method offers a simpler alternative to traditional metal-based reducing agents and may pave the way for applications in adaptive catalysis and sensor development.

Finally, we demonstrated that the catalytic activity of the NDI-containing catalyst **4** could be switched on and off by sequentially adding excess fluoride and $NO^+BF_4^-$. To the best of our knowledge, this is the first example of switchable catalysis based on a Pd(II)/Pd(IV) cycle. Furthermore, this sequence represents one of the rare instances of a halide-induced redox-switchable process, a phenomenon previously reported only once.[10]

Data availability

The datasets supporting this article have been uploaded as part of the ESI.†

Author contributions

S. Martínez-Vivas prepared the complexes and carried out all experimental work. M. Poyatos and E. Peris designed and supervised the study. All authors have given approval to the final version of the manuscript.

Conflicts of interest

There are no conflicts to declare.

Acknowledgements

We gratefully acknowledge financial support from the Ministerio de Ciencia y Universidades (PID2021-127862NB-I00) and the Universitat Jaume I (UJI-B2021-39). We are grateful to the Serveis Centrals d'Instrumentació Científica (SCIC-UJI) for providing spectroscopic facilities.

Notes and references

1 (*a*) A. J. Hickman and M. S. Sanford, *Nature*, 2012, **484**, 177; (*b*) J. J. Topczewski and M. S. Sanford, *Chem. Sci.*, 2015, **6**, 70; (*c*) P. Sehnal, R. J. K. Taylor and I. J. S. Fairlamb, *Chem. Rev.*, 2010, **110**, 824; (*d*) L. M. Xu, B. J. Li, Z. Yang and Z. J. Shi, *Chem. Soc. Rev.*, 2010, **39**, 712.

2 B. Zhang, X. C. Yan and S. Guo, *Chem.–Eur. J.*, 2020, **26**, 9430.

3 (*a*) A. S. McCall, H. W. Wang, J. M. Desper and S. Kraft, *J. Am. Chem. Soc.*, 2011, **133**, 1832; (*b*) A. S. McCall and S. Kraft, *Organometallics*, 2012, **31**, 3527; (*c*) T. Liang, C. N. Neumann and T. Ritter, *Angew. Chem., Int. Ed.*, 2013, **52**, 8214; (*d*) T. Furuya, A. S. Kamlet and T. Ritter, *Nature*, 2011, **473**, 470; (*e*) T. Furuya, H. M. Kaiser and T. Ritter, *Angew. Chem., Int. Ed.*, 2008, **47**, 5993; (*f*) T. Furuya and T. Ritter, *J. Am. Chem. Soc.*, 2008, **130**, 10060; (*g*) T. Furuya, D. Benitez, E. Tkatchouk, A. E. Strom, P. P. Tang, W. A. Goddard and T. Ritter, *J. Am. Chem. Soc.*, 2010, **132**, 3793.

4 (*a*) T. W. Lyons and M. S. Sanford, *Chem. Rev.*, 2010, **110**, 1147; (*b*) K. Yamamoto, J. K. Li, J. A. O. Garber, J. D. Rolfes, G. B. Boursalian, J. C. Borghs, C. Genicot, J. Jacq, M. van Gastel, F. Neese and T. Ritter, *Nature*, 2018, **554**, 511; (*c*) D. C. Powers, D. Y. Xiao, M. A. L. Geibel and T. Ritter, *J. Am. Chem. Soc.*, 2010, **132**, 14530.

5 (*a*) X. Yan, H. Wang and S. Guo, *Angew. Chem., Int. Ed.*, 2019, **58**, 16907; (*b*) M. Nappi and M. J. Gaunt, *Organometallics*, 2019, **38**, 143.

6 J. Vicente, A. Arcas, F. Julia-Hernandez and D. Bautista, *Inorg. Chem.*, 2011, **50**, 5339.

7 (*a*) H. B. Li, B. Zhang, R. Feng and S. Guo, *Dalton Trans.*, 2024, **53**, 11470; (*b*) D. C. Najera, G. E. Martinez and A. R. Fout, *Organometallics*, 2023, **42**, 832.

8 S. Martinez-Vivas, M. Poyatos and E. Peris, *Angew. Chem., Int. Ed.*, 2023, **62**, e202307198.

9 S. Martínez-Vivas, D. G. Gusev, M. Poyatos and E. Peris, *Angew. Chem., Int. Ed.*, 2023, **62**, e202313899.

10 S. Martínez-Vivas, S. Gonell, M. Poyatos and E. Peris, *ACS Catal.*, 2024, 7600.

11 (*a*) M. R. Ajayakumar, P. Mukhopadhyay, S. Yadav and S. Ghosh, *Org. Lett.*, 2010, **12**, 2646; (*b*) M. R. Ajayakumar, D. Asthana and P. Mukhopadhyay, *Org. Lett.*, 2012, **14**, 4822; (*c*) J. F. Zhao, G. Li, C. Y. Wang, W. Q. Chen, S. Chye, J. Loo and Q. C. Zhang, *RSC Adv.*, 2013, **3**, 9653; (*d*) A. Mitra, R. J. Clark, C. T. Hubley and S. Saha, *Supramol. Chem.*, 2014, **26**, 296; (*e*) M. Giese, M. Albrecht and K. Rissanen, *Chem. Commun.*, 2016, **52**, 1778; (*f*) Y. J. Zhao, Y. Cotelle, N. Sakai and S. Matile, *J. Am. Chem. Soc.*, 2016, **138**, 4270.

12 (*a*) S. Guha, F. S. Goodson, L. J. Corson and S. Saha, *J. Am. Chem. Soc.*, 2012, **134**, 13679; (*b*) G. Belanger-Chabot, A. Ali and F. P. Gabbai, *Angew. Chem., Int. Ed.*, 2017, **56**, 9958; (*c*) S. Saha, *Acc. Chem. Res.*, 2018, **51**, 2225; (*d*) B. Chowdhury, S. Sinha, R. Dutta, S. Mondal, S. Karmakar and P. Ghosh, *Inorg. Chem.*, 2020, **59**, 13371; (*e*) T. L. D. Tam and J. W. Xu, *Chem. Commun.*, 2019, **55**, 6225.

13 (*a*) K. L. Hull, E. L. Lanni and M. S. Sanford, *J. Am. Chem. Soc.*, 2006, **128**, 14047; (*b*) J. M. Racowski, A. R. Dick and M. S. Sanford, *J. Am. Chem. Soc.*, 2009, **131**, 10974; (*c*) F. Saito, H. Aiso, T. Kochi and F. Kakiuchi, *Organometallics*, 2014, **33**, 6704; (*d*) W. B. Liu, Y. Q. Zhu and C. J. Li, *Synthesis*, 2016, **48**, 1616; (*e*) J. Vána, J. Bartácek, J. Hanusek, J. Roithová and M. Sedlák, *J. Org. Chem.*, 2019, **84**, 12746; (*f*) S. R. Whitfield and M. S. Sanford, *J. Am. Chem. Soc.*, 2007, **129**, 15142.

14 (*a*) X. Chen, G. Dobereiner, X. S. Hao, R. Giri, N. Maugel and J. Q. Yu, *Tetrahedron*, 2009, **65**, 3085; (*b*) S. Strekalova, A. Kononov, I. Rizvanov and Y. Budnikova, *RSC Adv.*, 2021, **11**, 37540.

15 (*a*) X. Y. Guo, G. J. Deng and C. J. Li, *Adv. Synth. Catal.*, 2009, **351**, 2071; (*b*) T. Rogge and L. Ackermann, *Angew. Chem., Int.*

Ed., 2019, **58**, 15640; (*c*) M. Muntzeck, F. Pippert and R. Wilhelm, *Tetrahedron*, 2020, **76**, 131314.
16 Y. L. Xie, D. D. Xu, W. W. Sun, S. J. Zhang, X. P. Dong, B. Liu, Y. B. Zhou and B. Wu, *Asian J. Org. Chem.*, 2016, **5**, 961.
17 K. Yang, M. Song, A. I. M. Ali, S. M. Mudassir and H. Ge, *Chem.–Asian J.*, 2020, **15**, 729.
18 L. A. Wright, E. G. Hope, G. A. Solan, W. B. Cross and K. Singh, *Dalton Trans.*, 2015, **44**, 7230.